



## SEISMIC PROGRESSIVE COLLAPSE ANALYSIS ON REINFORCED CONCRETE BRIDGES

Hartanto Wibowo<sup>1</sup> and David T. Lau<sup>2</sup>

### ABSTRACT

Although there have been many studies in the area of progressive collapse of structures in recent years, most of these investigations focus on buildings collapse caused by blast loadings. The problem of progressive collapse of bridges during earthquakes is not as well understood. This paper presents results from a study on progressive collapse analysis of reinforced concrete bridges during earthquake that takes into account the effects of element separation and impact forces from falling debris. The computer simulation results illustrate details of the failure process from initial failure of individual component, progression and spread of damage, to ultimate collapse of the analyzed bridge structure. The results show that failure of a single structural component can have significant ramification effect that can drastically change the behaviour of the entire bridge system in a collapse process that is not well understood before. The analysis tools and better understanding of progressive collapse behaviour and performance of bridges can lead to more effective design and retrofit strategies by taking into account the expected post-earthquake damage of structures.

### Introduction

Progressive collapse of structures is a phenomenon in which an initial local failure spreads from structural element to other elements which eventually results in the collapse of the whole structure or to an extent disproportionate to the original failure. In seismic behaviour of structures, progressive collapse can be defined as a sequence of events starting from initiation of failure of a single component, due to overstress beyond the elastic limit, to degradation of material and member properties as related to stiffness and strength that are the result of accumulation of damage effects from cyclic stress reversals until the development of collapse mechanism. Experiences from past major earthquakes have shown that collapse of bridges can have catastrophic consequences, such as disruption to post-disaster rescue efforts and significant economic loss. In a number of post-earthquake reconnaissance studies of structural damage, the seismic performance of bridges during past earthquakes was deemed to be not satisfactory

---

<sup>1</sup> Graduate Research Assistant, Department of Civil and Environmental Engineering, University of Nevada - Reno, Reno, NV, 89557, USA (wibowoh@unr.nevada.edu)

<sup>2</sup> Professor and Director of Ottawa – Carleton Bridge Research Institute, Department of Civil and Environmental Engineering, Carleton University, Ottawa, ON, K1S 5B6, Canada (dtl@ccs.carleton.ca)

(Priestley *et al.* 1996, Kawashima 2000, Wallace *et al.* 2001, Buckle 2003, Moehle and Eberhard 2003, Han *et al.* 2009). In current practice of analysis and design of structures against earthquake effects, structures are designed to have the strength and deformation capacities to resist the demands of design earthquake. In ductile design of earthquake resistant structures, the ability of a structure to continue resisting severe ground shaking after initial failure that exceeds its elastic limit without significant loss of load carrying capacity depends on the amount of accumulated damage suffered by the structure. The impact of the accumulated damage and its influence on the overall seismic performance of bridge structures have not been investigated with proper detailed models and analyses.

To achieve the goal of better seismic performance of structures within the context of the Performance-Based Earthquake Engineering, it is necessary to have a thorough understanding of the complete structural response behaviour over the entire duration of seismic response from initial failure of individual structural components or members, progression of structural failure, and the influence of accumulated structural damage on the strength and stiffness of the structure to the final ultimate collapse of the structural system. To obtain insights and detailed information for improvements in understanding the seismic risk and vulnerability of structures, accurate prediction models and analysis tools are needed for determining the complete detailed inelastic behaviour and performance of structures during earthquakes. This paper presents results obtained from a study on seismic progressive collapse analysis of reinforced concrete bridges. A better understanding and insights on the seismic performance of bridges can lead to bridge design improvement, disaster risk reduction, and better emergency preparedness. More effective and performance-based design, retrofit, and mitigation strategies can be developed to help reducing the enormous cost required for renewing the existing old bridge infrastructures.

### Applied Element Method

The Applied Element Method (AEM), proposed by Tagel-Din and Meguro (1999), combines the advantages of both continuum analysis models (e.g., Finite Element Method) and discrete analysis models (e.g., Discrete Element Method). The modelling approach of the AEM can easily account for element separation and contact as well as impact load from falling debris which makes it suitable as a tool for progressive collapse analysis of structures.

In the AEM, a structure is modelled by dividing it into an assembly of small rigid elements connected by springs at interfaces between adjacent elements, as shown in Fig. 1. Two adjacent elements of the 2D planar frame structures as shown in Fig. 1 are connected at discrete points along the element interfaces by a pair of normal and shear springs with the stiffness,  $K_n$  and  $K_s$ , given respectively as follows (Meguro and Tagel-Din 2000):

$$K_n = \frac{E d t}{a} \quad \text{and} \quad K_s = \frac{G d t}{a} \quad (1)$$

where  $d$  is the distance between springs,  $t$  is the element thickness,  $a$  is the length of the representative area,  $E$  is the material Young's modulus, and  $G$  is the material shear modulus. The spring stiffness expressions in Eq. 1 are derived based on the assumption that the

deformations of the domain volume are represented by the spring deformations at the interface between the adjacent rigid elements with the dimensions  $d$ ,  $t$ , and  $a$ , as depicted by the shaded area in Fig. 1, subjected to given loading. In the case that reinforcement bar is present, rebar stiffness is added to the material stiffness in Eq. 1. Element rotation is resisted by a set of normal and shear springs. The contribution to rotational stiffness,  $K_r$ , from the normal springs can be calculated as follows (Meguro and Tagel-Din 2001):

$$K_r = \int_{z=-b/2}^{z=b/2} \frac{Et}{b} z^2 dz = \frac{Et b^2}{12} \quad (2)$$

where  $b$  is the element height and  $z$  is the distance from the spring location to the centroid of the element as shown in Fig. 2. In the formulation, the inelastic and nonlinear material behaviour and fracture failure of material are modelled by nonlinear stiffness properties and removal of the springs.

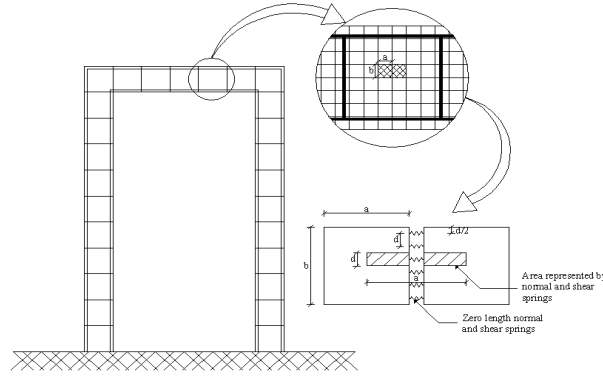


Figure 1. Elements on the applied element method

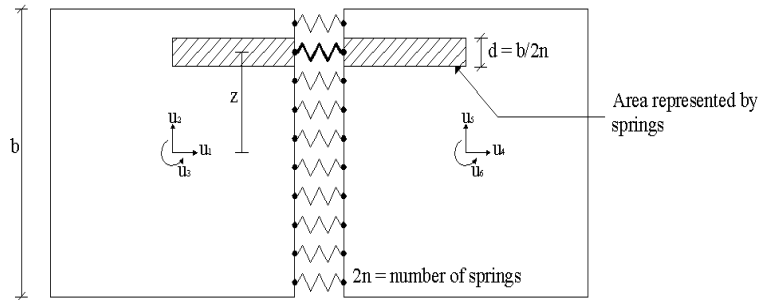


Figure 2. Normal springs for rotational stiffness calculation

In the AEM formulation, the general dynamic equation of motion in large deformation range is expressed as follows (Tagel-Din and Meguro 2000):

$$\mathbf{M} \Delta \ddot{\mathbf{U}} + \mathbf{C} \Delta \dot{\mathbf{U}} + \mathbf{K} \Delta \mathbf{U} = \Delta \mathbf{f}(t) + \mathbf{R}_M + \mathbf{R}_G \quad (3)$$

where  $\mathbf{M}$  is the mass matrix,  $\mathbf{C}$  is the damping matrix,  $\mathbf{K}$  is the nonlinear stiffness matrix, and  $\Delta \mathbf{f}(t)$  is the incremental applied load vector for a time step.  $\Delta \mathbf{U}$ ,  $\Delta \dot{\mathbf{U}}$ , and  $\Delta \ddot{\mathbf{U}}$  are the incremental displacement, velocity, and acceleration vectors respectively.  $\mathbf{R}_M$  is the additional load vector due to the nonlinear behaviour of material and  $\mathbf{R}_G$  is the additional load vector due to geometrical changes. Eq. 3 represents the equilibrium equation between the applied external forces and the internal forces. The solution of Eq. 3 can be obtained by numerical direct integration technique and in this case the Newmark's average acceleration method is chosen. Some verification examples can be found in Wibowo *et al.* (2009) and Wibowo (2009).

To follow the behaviour of concrete under compression, the Maekawa compression model (Okamura and Maekawa 1991) that describes the loading, unloading, and reloading conditions, is adopted. For modelling concrete subjected to tension, an initial stiffness is assumed for the concrete springs until they reach the cracking point. After cracking, the spring stiffness is set to zero. The steel reinforcement material model used is the Ristic model (Ristic *et al.* 1986) that considers the effects of partial unloading and the Bauschinger's effect. The failure criteria are based on the principal stresses in the springs so the proper crack propagation can be followed. When the stress in a spring exceeds the critical value of the tensile resistance, the normal and shear spring forces are redistributed so that the tension stress is zero on the crack face.

### Bridge Model

The example bridge used in the present study has four 20 m bays with a total length of 80 m. The bridge superstructure dimensions and pier heights of 5.6 m, 2.8 m, and 8.4 m respectively, as shown in Fig. 3. The pier base is modelled as fixed at the pier bases (Piers 2 to 4) and hinged at the abutments (1 and 5). The longitudinal reinforcement details of the bridge are taken from the bridge model used in the study by Casarotti and Pinho (2006). In the present study, the transverse reinforcement details of the piers are determined based on the design requirements of CAN/CSA-S6-06 (CSA 2006). The bridge superstructure is a box girder 5.6 m wide and in this study, the girder is considered as reinforced concrete girder. The bridge box girder has minimum transverse reinforcements. The bridge substructures are rectangular hollow-core reinforced concrete piers. The connection between the pier and the box girder is assumed as pin, which does not transfer any moment between the box girder and the pier. The bridge's piers properties are summarized in Table 1. In the applied element model, the bridge box girder is modelled to remain elastic during earthquake response in the comparison study with previous analytical and experimental test results where elastic bridge superstructure is assumed (Casarotti and Pinho 2006). The concrete and steel properties are tabulated in Table 1. The damping ratio of the bridge in the analysis is taken as 5%.

The longitudinal reinforcement details of the bridge box girder are shown in Fig. 4(a). The box girder is designed such that it matches the moment of inertia specified in the literature (Casarotti and Pinho 2006). The piers' longitudinal reinforcement details are divided into two types. The 2.8 m high pier follows the reinforcement detail type 1, whereas the 5.6 m high and 8.4 m high piers follow the reinforcement detail type 2. The longitudinal reinforcement details of the piers are shown in Fig. 4(b).

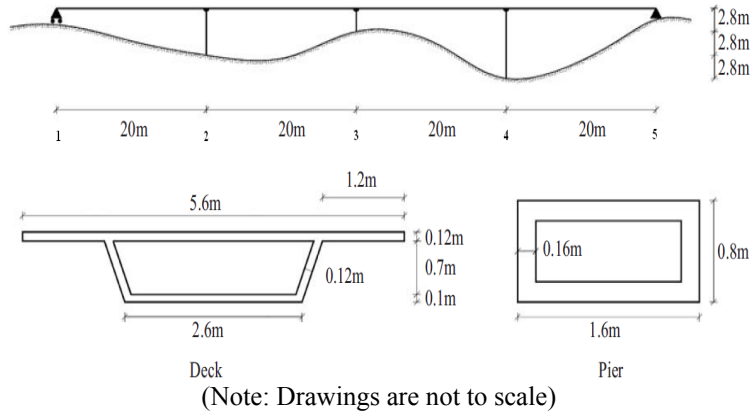


Figure 3. Bridge model elevation view and sections (Casarotti and Pinho 2006)

Table 1. Properties of the bridge model (Casarotti and Pinho 2006)

<i>Parameter</i>	<i>Concrete</i>			<i>Steel</i>
	<i>Pier 2</i>	<i>Pier 3</i>	<i>Pier 4</i>	
<i>Compressive Strength</i>	$3.212 \times 10^6 \text{ kg/m}^2$	$3.569 \times 10^6 \text{ kg/m}^2$	$4.375 \times 10^6 \text{ kg/m}^2$	$3.6 \times 10^7 \text{ kg/m}^2$
<i>Tensile Strength</i>	$3.212 \times 10^5 \text{ kg/m}^2$	$3.569 \times 10^5 \text{ kg/m}^2$	$4.375 \times 10^5 \text{ kg/m}^2$	$3.6 \times 10^7 \text{ kg/m}^2$
<i>Strain at Unconfined Peak Stress</i>	0.002 m/m	0.002 m/m	0.002 m/m	-
<i>Constant Confinement Factor</i>	1.2	1.2	1.2	-
<i>Young's Modulus</i>	$2.549 \times 10^9 \text{ kg/m}^2$	$2.549 \times 10^9 \text{ kg/m}^2$	$2.549 \times 10^9 \text{ kg/m}^2$	$2.0389 \times 10^{10} \text{ kg/m}^2$
<i>Shear Modulus</i>	$1.062 \times 10^9 \text{ kg/m}^2$	$1.062 \times 10^9 \text{ kg/m}^2$	$1.062 \times 10^9 \text{ kg/m}^2$	$8.15561 \times 10^9 \text{ kg/m}^2$
<i>Specific Weight</i>	$2549.291 \text{ kg/m}^3$	$2549.291 \text{ kg/m}^3$	$2549.291 \text{ kg/m}^3$	$7840 \text{ kg/m}^3$
<i>Separation Strain</i>	0.1	0.1	0.1	0.2
<i>Friction Coefficient</i>	0.8	0.8	0.8	0.8
<i>Post-yield Stiffness Ratio</i>	-	-	-	0.01

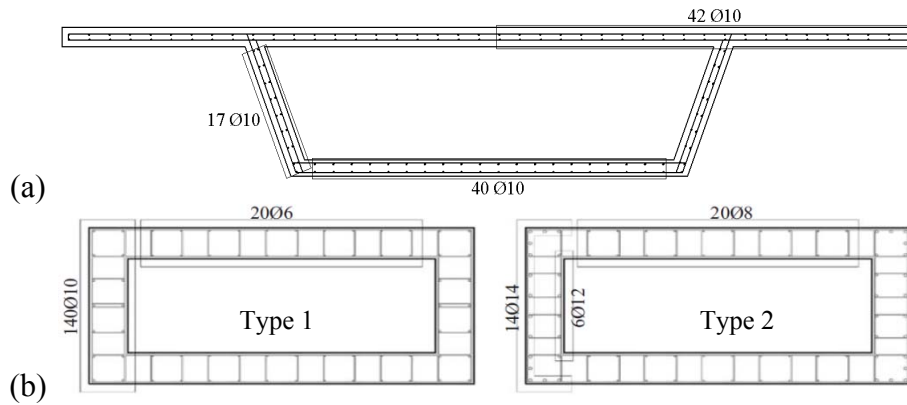


Figure 4. (a) Box girder and (b) piers (Casarotti and Pinho 2006) longitudinal reinforcement details

In the applied element model of the bridge, each side of the pier cross-section is divided into a mesh of 5 x 5 equal spaced elements and in the longitudinal direction into 5 equal spaced elements per 2.8 m length. Each surface area of the box girder section (i.e., the deck, webs, and soffit) is divided into 10 x 1 elements with 50 elements per 20 m length in the longitudinal direction of the box girder. This mesh size has been found to give accurate results. Analysis using a finer mesh has been carried out without any noticeable difference in the numerical results.

### Earthquake Ground Motions

Earthquake ground motion records used in the analysis are obtained from the Pacific Earthquake Engineering Research (PEER) Strong Motion Database. The earthquake records used are the 1994 Northridge, the 1995 Kobe, and the 1999 Chi-Chi earthquake records. The earthquake excitation is applied in the longitudinal (x-axis), transversal (y-axis), and vertical (z-axis) directions. A summary of the earthquake ground motions is presented in Table 2.

Table 2. Summary of the earthquake ground motions

<i>Earthquake Name</i>	<i>Peak Ground Acceleration</i>			<i>Duration</i>
	<i>X-Direction</i>	<i>Y-Direction</i>	<i>Z-Direction</i>	
<i>1994 Northridge</i>	1.585 g	1.285 g	1.229 g	40.00 s
<i>1995 Kobe</i>	0.821 g	0.599 g	0.343 g	48.00 s
<i>1999 Chi-Chi</i>	0.821 g	0.653 g	0.337 g	360.00 s

### Results and Discussion

The progression of the structural failure and collapse of the analyzed bridge due to the 1994 Northridge, the 1995 Kobe, and the 1999 Chi-Chi earthquakes are captured in Figs. 5 to 7, respectively. From observation, it can be noticed that the 1999 Chi-Chi earthquake caused the most damage to the bridge structure. Due to this earthquake, the box girder starts to fail early in the response and that actuates the short pier to bear more loads beyond its capacity and thus leads to its subsequent failure. The short pier collapses in flexure since it attracts the most seismic force. This short pier collapse also greatly reduces the load resistant capacity of the bridge resulting in the ramification effect of load shifts in the whole system which finally leads to the tall pier collapses. The collapse of the pier can also happen as a result of impact force from the failure of the box girder as can be observed in the collapse of the tall pier due to the 1995 Kobe earthquake.

The pier can also experience permanent deformation caused by the tilting and dislocation of the pier. Fig. 8 shows an example of dislocation and cracks in the pier due to the 1995 Kobe earthquake excitation, where a part of the short pier is no longer completely intact at the base. The displacement time histories along the x-axis at the top of the piers caused by the 1995 Kobe are shown in Fig. 9. The collapse of the girder results in the pier losing its lateral bracing

support, then it displaces more from the dragging action of the falling girder before it is completely separated from the pier during the response. The internal forces of the piers due to the three earthquakes can be found in Wibowo (2009). Although not presented here, the internal forces also have the same patterns as the displacements. The jumps in the internal forces occur when the abutments fail and the loads from the box girder are transferred fully to the piers and when there are impact forces from the debris.

In comparing the effects of different earthquake ground motions on the progressive collapse behaviour, it is noted that the 1994 Northridge earthquake excitation with the highest peak ground acceleration causes no pier to collapse but the 1999 Chi-Chi earthquake excitation causes significant collapse or failures of the entire bridge structures including the piers. The response spectrum of the 1999 Chi-Chi earthquake ground motion show that its frequency content has higher energy in longer period range compared to the 1994 Northridge earthquake. Since the bridge softens due to strength or stiffness deteriorations after structural members start to fail and suffer damage, the period shifts in the structure to longer due to its softening and makes it more vulnerable to more severe earthquake damage.

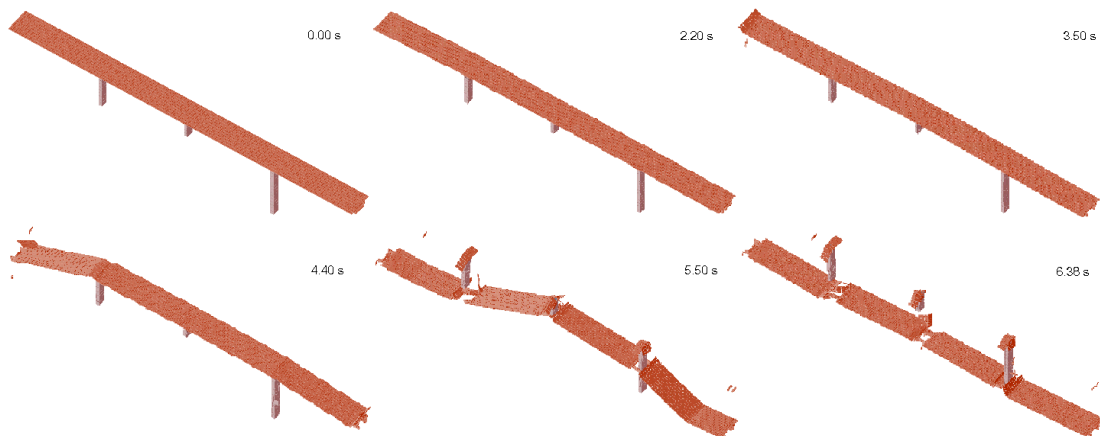


Figure 5. Progression of collapse due to the 1994 Northridge earthquake excitation

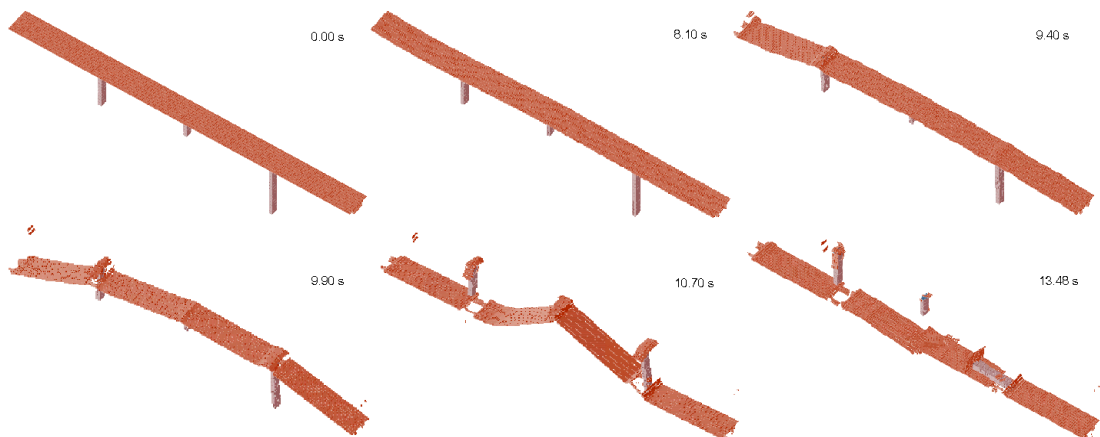


Figure 6. Progression of collapse due to the 1995 Kobe earthquake excitation

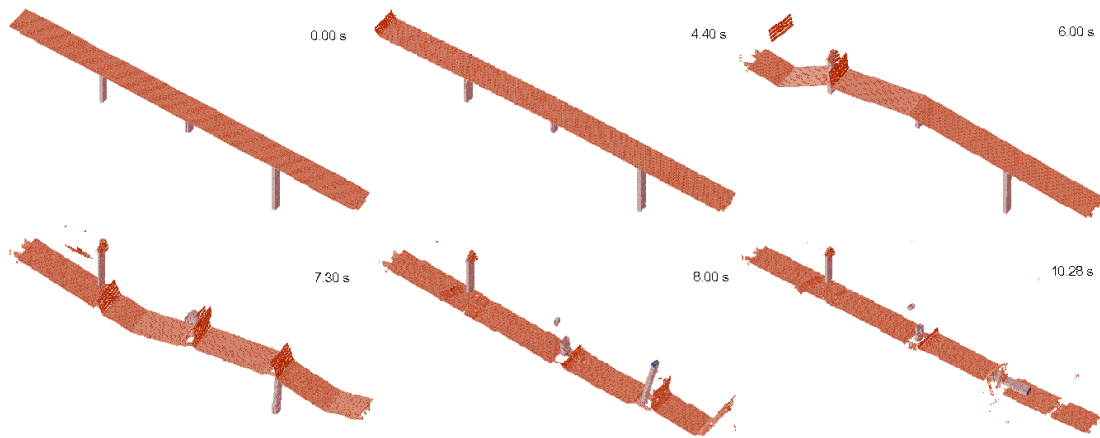


Figure 7. Progression of collapse due to the 1999 Chi-Chi earthquake excitation

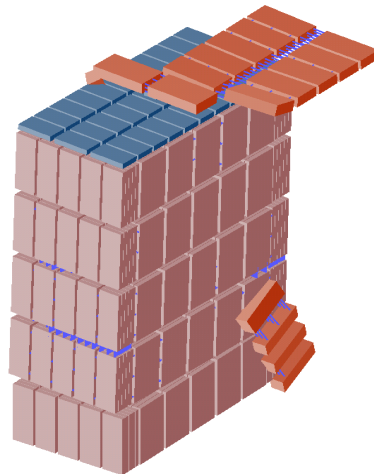


Figure 8. Dislocation and cracks of the short pier due to the 1995 Kobe earthquake excitation

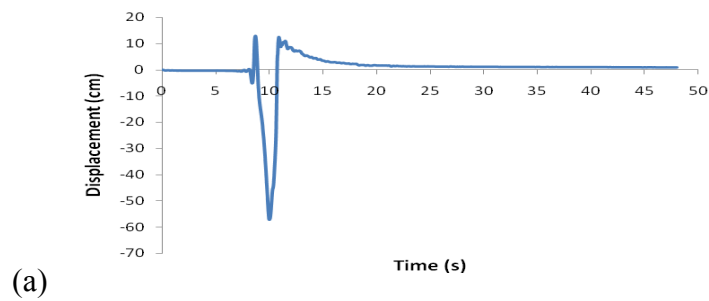


Figure 9. (a) Short pier's top displacement time history along the x-axis due to the 1995 Kobe earthquake excitation

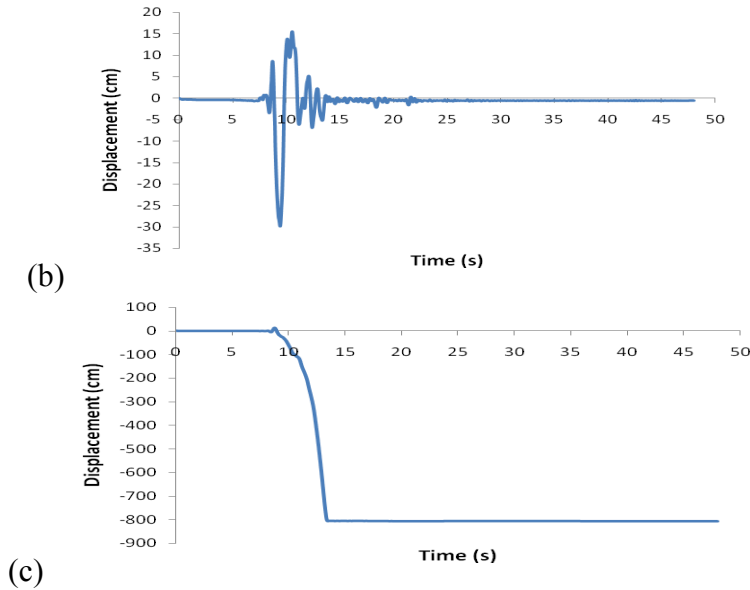


Figure 9. (cont'd) (b) Medium and (c) tall piers' top displacement time histories along the x-axis due to the 1995 Kobe earthquake excitation

### Conclusions

The analysis results show that seismic progressive collapse phenomenon is global damage behaviour of the structure. During earthquakes, part of a structure starts to fail causing redistribution of load to the remainder of the structural system and subsequent failure and development of collapse mechanisms. The response of structures during the collapse process is highly nonlinear and influenced by the response from impact force of falling debris. There are drastic changes in mass, strength, and stiffness properties of the structure during the progressive collapse process. Progressive collapse phenomena should be considered in the seismic design of structures to increase safety. Seismic progressive collapse simulations can help structural engineers to better understand the design objective in performance-based seismic design of structures, including a more comprehensive approach in devising effective retrofit strategies for old deficient bridges by considering the pattern and severity of the potential damage in the structure.

### Acknowledgments

The authors would like to acknowledge Dr. Hatem Tagel-Din and Mr. Ayman El-Fouly of Applied Science International, LLC for the fruitful discussion and technical support of the software ELS. Prof. Rui Pinho of the University of Pavia is also indebted for providing the reinforcement details of the bridge model. This research is a part of the NSERC Strategic Network Grant Project: Canadian Seismic Research Network.

### References

Buckle, I. G., 2003. Application of seismic risk assessment procedures to the performance-based design of highway systems, *Advancing Mitigation Technologies and Disaster Response for Lifeline*

- Systems*, Beavers, J. E. (ed.), 886-895.
- Canadian Standards Association (CSA), 2006. *CAN/CSA-S6-06 Canadian Highway Bridge Design Code*, CSA International, Toronto, ON.
- Casarotti, C. and R. Pinho, 2006. Seismic response of continuous span bridges through fiber-based finite element analysis, *Earthquake Engineering and Engineering Vibration* 5 (1), 119-131.
- Han, Q., X. Du, J. Liu, Z. Li, L. Li, and J. Zhao, 2009. Seismic damage of highway bridges during the 2008 Wenchuan earthquake, *Earthquake Engineering and Engineering Vibration* 8 (2), 263-273.
- Kawashima, K., 2000. Seismic performance of RC bridge piers in Japan: An evaluation after the 1995 Hyogo-ken Nanbu earthquake, *Progress in Structural Engineering and Materials* 2 (1), 82-91.
- Meguro, K. and H. Tagel-Din, 2000. Applied element method for structural analysis: Theory and application for linear materials, *Structural Engineering/Earthquake Engineering JSCE* 17 (1), 21s-35s.
- Meguro, K. and H. Tagel-Din, 2001. Applied element simulation of RC structures under cyclic loading, *Journal of Structural Engineering ASCE* 127 (11), 1295-1305.
- Moehle, J. P. and M. O. Eberhard, 2003. Earthquake damage to bridges, *Bridge Engineering: Seismic Design*, Chen, W. -F. and L. Duan (eds.), 33 pp.
- Okamura, H. and K. Maekawa, 1991. *Nonlinear Analysis and Constitutive Models of Reinforced Concrete*, Gihodo Co. Ltd., Tokyo.
- Priestley, M. J. N., F. Seible, and G. M. Calvi, 1996. *Seismic Design and Retrofit of Bridges*, John Wiley & Sons Inc., New York, NY.
- Ristic, D., Y. Yamada, and H. Iemura, 1986. *Stress-strain Based Modeling of Hysteretic Structures under Earthquake Induced Bending and Varying Axial Loads*, Research Report No. 86-ST-01, School of Civil Engineering, Kyoto University, Kyoto, Japan.
- Tagel-Din, H. and K. Meguro, 1999. Applied element simulation for collapse analysis of structures, *Bulletin of Earthquake Resistant Structure Research Center* 32, 11 pp.
- Tagel-Din, H. and K. Meguro, 2000. Applied element method for dynamic large deformation analysis of structures, *Structural Engineering/Earthquake Engineering JSCE* 17 (2), 215s-224s.
- Wallace, J. W., M. O. Eberhard, S. -J. Hwang, J. P. Moehle, T. Post, C. Roblee, J. P. Stewart, and M. Yashinsky, 2001. Highway bridges, *Earthquake Spectra: Chi-Chi Earthquake Reconnaissance Report* 17 (S1), 131-152.
- Wibowo, H., 2009. Progressive collapse analysis of reinforced concrete bridges during earthquakes, *M.A.Sc. Thesis*, Carleton University, Ottawa, ON, Canada.
- Wibowo, H., S. S. Reshotkina, and D. T. Lau, 2009. Modelling progressive collapse of RC bridges during earthquakes. *Proceedings of CSCE Annual General Conference 2009: On the Leading Edge*, Paper No. GC-176, 11 pp.